

# CARBURIZING-QUENCHING HARDNESS MODEL ANALYSIS AND COMPARISON

## MODELNA ANALIZA IN PRIMERJAVA MODELA ZA NAPOVED TRDOTE JEKLA DOSEŽENE S POSTOPKOM NAOGLJICENJA IN KALJENJA

Wang Xin

Mechanical Engineering College, Henan University of Engineering, Zhengzhou, PR China

*Prejem rokopisa – received: 2023-09-23; sprejem za objavo – accepted for publication: 2023-11-13*

doi:10.17222/mit.2023.978

Unlike the conventional calculation models of the hardness, a carburizing-quenching hardness model considers the influence of the carbon content on the phase transformation and hardness. The volume fraction model (VFM) and Jominy curve model (JCM) for calculating carburizing-quenching hardness of 20CrNi2Mo steel were built in this study, and the models were used to calculate the hardness of Jominy and gear samples. The hardness results of both models were compared, and the simulation results were verified with the corresponding test results. The results show that the hardness values obtained with both models have a certain calculation accuracy. But due to considering the influence of residual austenite (RA) on the hardness, the simulation accuracy of the VFM was better for the low Jominy distance and the hardened case, while the simulation accuracy of the JCM was better for the large Jominy distance and the low-carbon martensite region; the calculation of the latter is more convenient and its accumulated error is small.

Keywords: carburizing-quenching, Jominy distance, carbon content, hardness

V modelu za napoved trdote jekla z naogljicjenjem in kaljenjem je potrebno izvesti primerjavo s konvencionalnimi modeli za izračun trdote, kiupoštevajo vsebnost ogljika in fazne transformacije. V tem članku avtor opisuje izdelavo modela volumskega deleža (VFM, angl.: Volume Fraction Model) in modela Jominy krivulj (JCM, angl.: Jominy curve model) za izračun trdote jekla za zobnike vrste 20CrNi2Mo po naogljicjenju in kaljenju. Modela je nato avtor verificiral z Jominyjevim preizkusom in na vzorcih zobnikov. Med seboj je primerjal oba modela. Rezultati primerjav med obema modeloma so pokazali dokaj dobro natančnost izračunov. Toda zaradi upoštevanja vpliva vsebnosti zaostalega austenita (RA, angl.: residual austenite) na trdoto je bila natančnost simulacije z VFM modelom boljša pri manjših Jominy oddaljenostih od hlajene ploskve preizkušanca. Boljša natančnost JCM modela pa je bila pri večjih Jominy oddaljenostih od hlajene površine preizkušancev in pri področjih z manjšo vsebnostjo ogljika v martenzitu. Tako se je izkazalo, da je ta model kumulativno ugodnejši za izračunavanje trdote in ima v celoti manjšo napako.

Ključne besede: naogljicjenje in kaljenje, Jominy razdalja, vsebnost ogljika, trdota

## 1 INTRODUCTION

Carburization-quenching can improve the surface hardness and wear resistance of a sample. It is very important to obtain the core and surface hardness distribution of parts exposed to carburizing-quenching.<sup>1,2</sup> In order to avoid time-consuming process optimization, it is important to build an accurate hardness prediction model. At present, there are mainly two models for hardness calculation, namely the VFM and JCM.<sup>3-5</sup> The VFM can simulate a nonhomogeneous microstructure field, and confirm the hardness of the microstructure. Doane et al.<sup>6</sup> indicated that the method is only suitable when the carbon content is lower than 0.5 %. Wood et al.<sup>7</sup> predicted the quenching hardness by simulating the temperature and microstructure fields of a steel cylinder, taking the hardness of RA as being equal to the hardness of martensite. Yuan et al.<sup>8</sup> summed up some formulas for the calculation of martensite hardness, and predicted the

hardness by simulating the martensite transformation. Zhang et al.<sup>9</sup> predicted the carburizing-quenching hardness by considering the effects of RA and the carbon content on the martensite hardness. But this method can only show the hardness of a discrete point. The distribution of the hardness field cannot be presented as a shaded display and easily extracted. Schwenk et al.<sup>10</sup> calculated the hardness depth for spur or bevel gears, considering all physical aspects of the carburizing and quenching process with the VFM. During the simulation, geometric approximation of gears ensured the accuracy of carburizing and hardness calculations.

The JCM predicts the hardness based on the Jominy hardness curve and Jominy cooling curve.<sup>11</sup> Ko et al.<sup>12</sup> predicted the hardness of an A16061 steel cylinder in the quenching process with the QFA (quench factor analysis). The predicted hardness was in a good agreement with the experimental hardness. But this model only calculated the hardness of a discrete point, and the extraction of the result was inconvenient. Kianezhad et al.<sup>13</sup> improved the QFA method, based on the work by Rometsch

\*Corresponding author's e-mail:  
haiyang630@163.com (Wang Xin)

et al.,<sup>14</sup> experimentally proving a higher efficiency of the new method. Moreover, Kianezhad et al.<sup>15</sup> predicted the hardness of quenched steel parts using the QFA and ANNs (artificial neural networks), and pointed out that the accuracy of the QFA was limited to the dominant structure. Wang et al.<sup>16</sup> summed up some formulas for the Jominy hardness. These formulas were only applicable to a carbon content of less than 0.56 %. Wang et al.<sup>11</sup> built an improved JCM for the carburizing-quenching process, but did not consider the influence of RA on the quenching hardness. The above studies mostly focused on a hardness prediction model, and there is little analysis or comparison of both models in terms of the principle and effectiveness. In the present study, the VFM and JCM of 20CrNi2Mo steel were built. Both models were used for the hardness calculation of Jominy and gear samples using DEFORM\_V11. The corresponding test results were utilized to verify the simulation results, and the simulation accuracy of both models was analysed and discussed.

**2 EXPERIMENTAL PROCEDURE**

Standard Jominy and three-tooth gear samples were prepared for the experiment and analysis, as shown in **Figure 1**. The experiment material was 20CrNi2Mo steel, and its composition is shown in **Table 1**. A quarter of the Jominy model and a half of a single tooth model were built as symmetric models. The mesh of the Jominy model in the length direction was refined. The carburizing process for both the Jominy and gear samples was the same. The carburizing was carried out in two stages, boost and diffusion, where the temperature was 930 °C while the carbon potentials and times were 1.15 for 22 h and 0.85 for 5.75 h. The carbon content was tested with an X-350A spectrometer. The carburized Jominy samples were subjected to the Jominy test where the heating temperature was 820 °C. Finally, the hardness of 12

points on the two axial planes were tracked and measured within 60 mm from the water-cooled end. The quenching temperature of the gear was 830 °C; the gear was immersed in quenching oil at 60 °C for 0.5 h. The hardness within 60 mm was tracked and tested in the addendum and dedendum.

**Table 1:** Composition of 20CrNi2Mo

Element	C	Mn	Ni	Si	Cr	Mo
w/%	0.20	0.47	1.80	0.16	0.53	0.24

**3 VFM AND JCM**

Carbon diffusion can be described with Fick’s law, according to which the transfer coefficient is 0.0001123 mm/s when the temperature is 930 °C.<sup>17</sup> In addition to considering the influence of the temperature and carbon content, with the calculation of the diffusion coefficient (*D*), the effect coefficient of alloying elements is also considered to ensure the calculation accuracy,<sup>18,19</sup> as shown below:

$$D = \left( 0.0047 \exp(-16C) \exp\left[\frac{-(37000 - 6600C)}{RT}\right] \right) \times \left( 0.013Mn + 0.013Mo + 0.040Cr - 0.055Si - 0.014Ni \right) \tag{1}$$

where *T* and *C* denote the temperature and carbon content, and each element denotes its mass percentage, as shown in **Table 1**. *R* is the gas constant.

The VFM hardness is calculated with the linear mixing principle,<sup>20</sup> as follows:

$$HRC_e = \sum V_i HRC_i \tag{2}$$

where *HRC<sub>e</sub>* is the Rockwell hardness of an element while *V<sub>i</sub>* and *HRC<sub>i</sub>* are the volume fraction and Rockwell hardness of the phase, respectively. The VFM

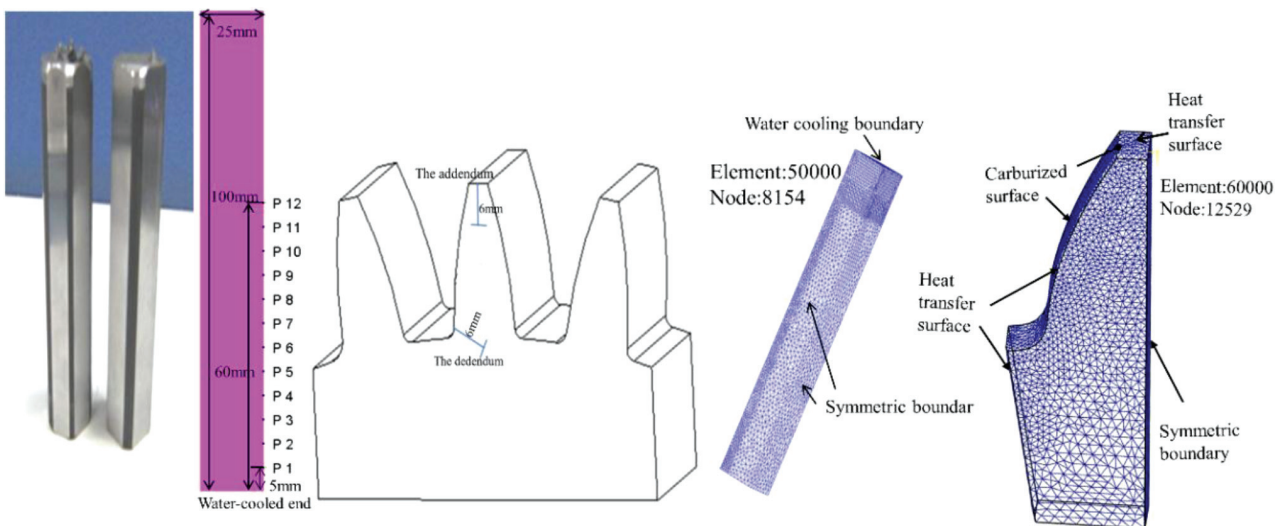


**Figure 1:** Jominy and gear sample

calculates the volume fraction and hardness of each element and then estimates the hardness based on the linear mixing principle. The volume fraction calculation is divided into the diffusive transformation and martensite transformation in the carburizing-quenching process. The former is calculated by the KJMA model based on

TTT curves.<sup>21,22</sup> Considering the influence of the carbon content, all the TTT curves are calculated by JMatPro, as shown in **Figure 2**. With an increase in the carbon content, the TTT curves of bainite and ferrite shift to the right and the transformation temperature decreases. The carbon content has little influence on the pearlite transformation.

Martensite transformation is calculated with the Koistinen-Marburger equation,<sup>23,24</sup> as shown in Equation (3), wherein the martensite transformation temperature ( $M_s$ ) under different carbon contents is calculated with Equation 4.<sup>25</sup>

$$V_M = 1 - \exp(-\alpha(M_s - T)) \quad (3)$$

$$M_s = 548 - 440C - (26Mn + 14Si + 14Ni + 11Cr + 9Mo) \quad (4)$$

Here,  $V_M$  is the martensite content while  $\alpha$  is taken as 0.011.

The hardness of pearlite, ferrite, bainite and martensite with a carbon content of less than 0.5 % is calculated based on the Maynier equation,<sup>9</sup> as shown below.

The Vickers hardness of ferrite and pearlite ( $HV_{F-P}$ ) is

$$HV_{(F-P)} = 42 + 223C + 53Si + 30Mn + 12.6Ni + 7Cr + 19Mo + (10 - 19Si + 4Ni + 8Cr + 130V) \log V_{(F-P)} \quad (5)$$

The Vickers hardness of bainite ( $HV_B$ ) is

$$HV_B = -323 + 185C + 330Si + 153Mn + 65Ni + 144Cr + 191Mo + (89 + 53C - 55Si - 22Mn - 10Ni - 20Cr - 33Mo) \log V_B \quad (6)$$

The Vickers hardness of martensite  $HV_M$  is

$$HV_M = 127 + 949C + 27Si + 11Mn + 8Ni + 16Cr + 21 \log V_M \quad (7)$$

$V_{F-P}$ ,  $V_B$  and  $V_M$  are critical cooling rates of each phase, respectively. The calculating equations are as follows:

$$\lg V_{(F-P)} = 6.36 - (0.43C + 0.49Mn + 0.78Ni + 0.26Cr + 0.301P_A) \quad (8)$$

$$\lg V_B = 10.17 - (3.8C + 1.07Mn + 0.7Ni + 0.57Cr + 1.58Mo + 0.00321P_A) \quad (9)$$

$$\lg V_M = 9.81 - (4.62C + 1.1Mn + 0.54Ni + 0.5Cr + 0.6Mo + 0.001831P_A) \quad (10)$$

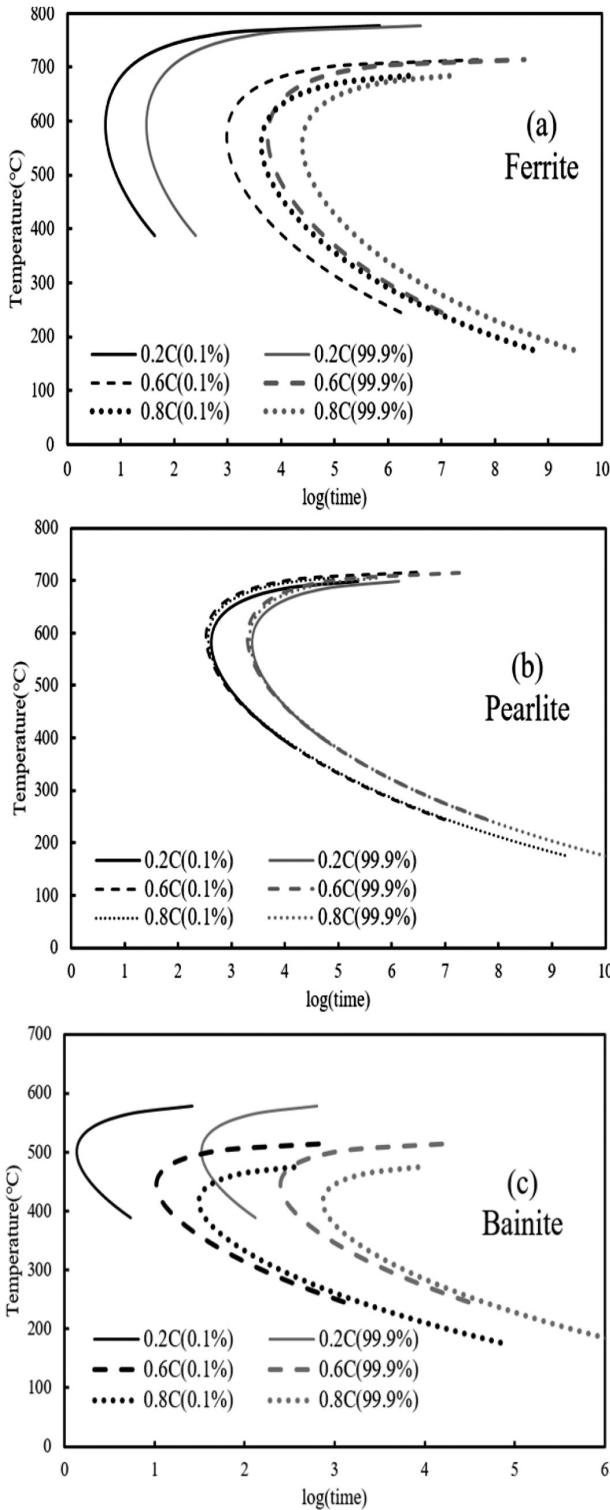


**Figure 2:** TTT curves of the diffusive transformation

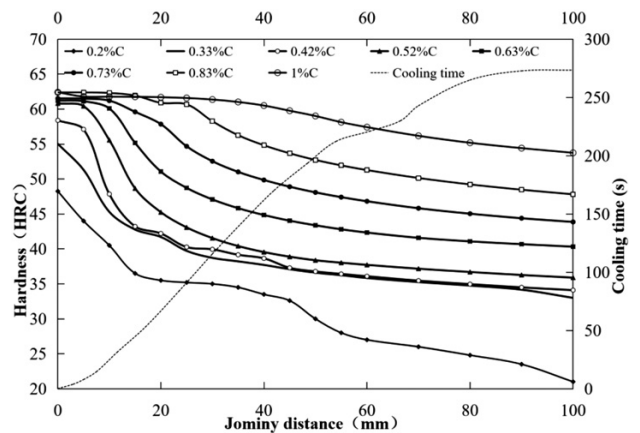


**Figure 3:** Jominy hardness curve and cooling curve

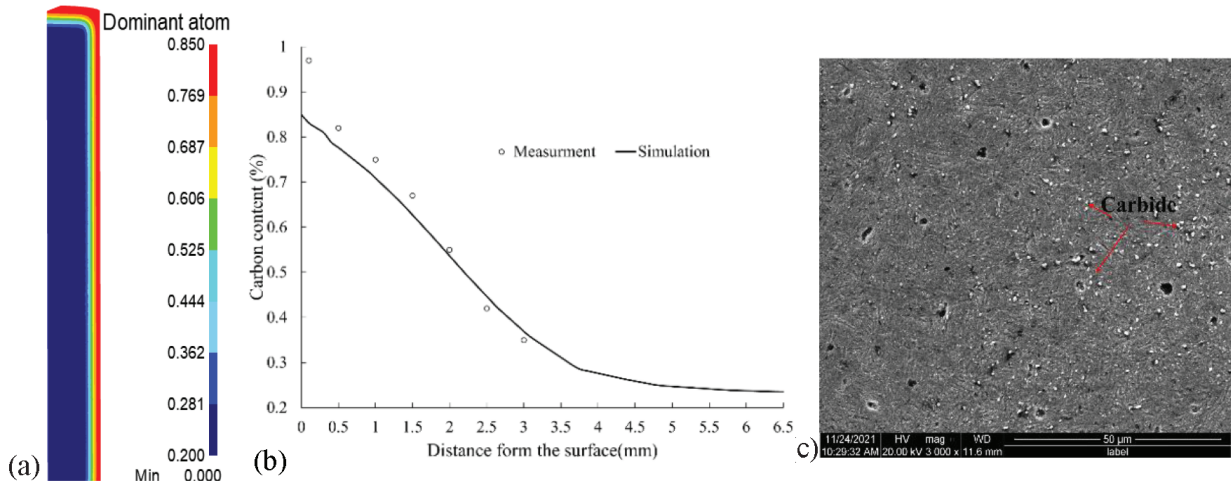


Figure 4: Carbon content of the Jominy sample: a) shade display, b) carbon content distribution curve, c) SEM micrograph

Here,  $P_A$  is equal to the product of the heating time and heating temperature. The calculated Vickers hardness of each phase can be converted to Rockwell hardness. The hardness of RA is equal to that of ferrite.

The martensite hardness with the carbon content of more than 0.5 % is only related to the carbon content,<sup>26</sup> calculated with Equation (11).

$$HRC_M = \frac{4 + 213C^3}{0.1 + 3.2C^3} - 2C + 15 \quad (c > 0.5 \%) \quad (11)$$

Jominy hardness curve and Jominy cooling curve are obtained with the JCM. Each cooling time corresponds to a Jominy distance in the Jominy cooling curve, and each Jominy distance corresponds to a Jominy hardness in the Jominy hardness curve; the cooling time and Jominy hardness mutually correspond based on the two curves. So when the cooling time of an element is calculated, the corresponding Jominy hardness is the hardness value of the element. Due to the carbon gradient in the carburizing case, the JCM should consider the influence of the carbon content on the hardness. So it should calculate the Jominy hardness curve for different carbon contents. The Jominy hardness curve of 20CrNi2Mo steel with the initial carbon content (0.2 %) was obtained based on the experiment result.<sup>27</sup> For the other carbon content, the hardness of Jominy distance within 40 mm is calculated with the USS-Atlas formula,<sup>11</sup> and the residual Jominy hardness is obtained with JmatPro. The Jominy cooling time is the representative cooling time of most alloy steels, that is, the cooling time of 820–500 °C ( $t_{8/5}$ ).<sup>28</sup> The  $t_{8/5}$  at different locations of the Jominy sample was obtained based on the temperature field of the Jominy sample. The Jominy hardness and cooling curve are shown in Figure 3. With the increasing carbon content, the Jominy hardness is also gradually improved. However, when the carbon content is greater than 0.63 %, the Jominy hardness of the low Jominy distance is slightly different. So when the cooling time and carbon content of an element are calculated, the correspond-

ing Jominy hardness in Figure 3 is the hardness of the element.

## 4 RESULTS AND DISCUSSION

### 4.1 Carbon content distribution

The simulated results of the carbon content for the Jominy sample are shown in Figure 4. The maximum carbon content is located on the surface of the sample, with a value of 0.85 %. The experiment result for the maximum carbon content on the surface was 0.97 %, which was significantly higher than the simulation. The material had a certain saturated carbon concentration, and under a high carbon potential during the boost stage, a certain amount of carbides occurred on the surface, resulting in a higher surface carbon content. The SEM micrograph of the sample surface in Figure 4c shows an obvious distribution of carbide particles. However, the carburizing simulation did not consider the carbide; it only considered the carbon diffusion in austenite, so the experiment results for the surface were significantly higher than the simulated results. But when the distance from the surface was greater than 0.5 mm, the measured and simulated results were in good agreement, and the

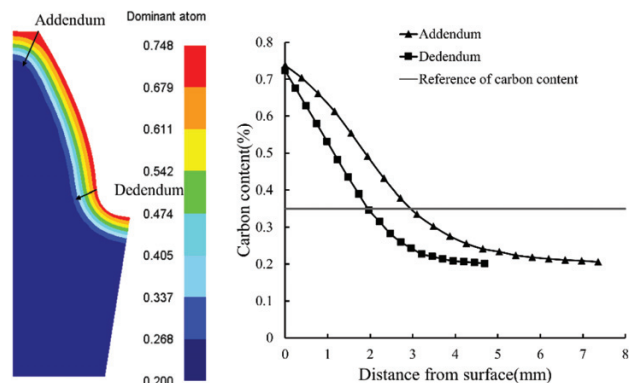


Figure 5: Carbon content of the gear

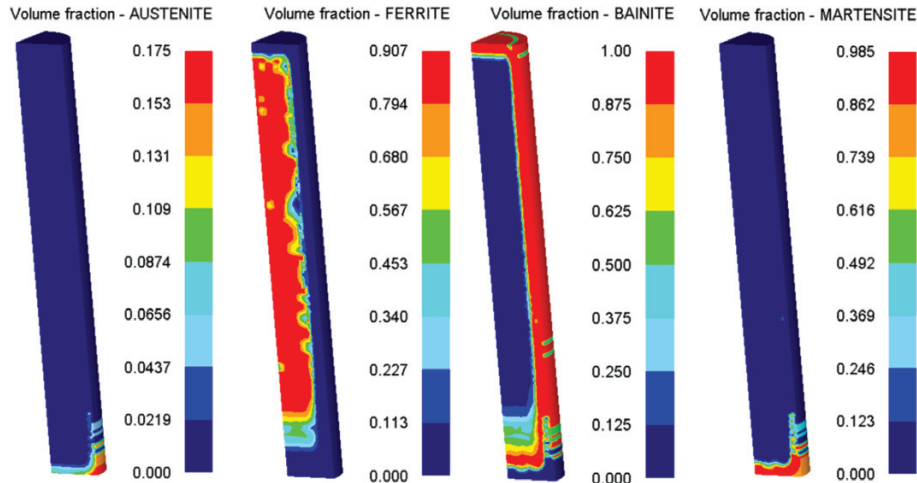


Figure 6: Phase transformation of the Jominy test

maximum difference between the simulated and measured results was 0.04 %.

The simulated results for the carbon content on the gear are shown in Figure 5. The maximum carbon content is located on the surface of the gear, and the maximum value is 0.748 %. Due to convex and concave shapes, the addendum region has the highest carbon content. The distance from the surface to the carbon content of 0.35 % defines the hardened area, which is about 2–3 mm at the addendum and dedendum.

#### 4.2 Phase transformation results

The phase transformation results for the carburized Jominy sample are shown in Figure 6. Martensite transformation mainly occurs in the J5 (distance from the water-cooled end) region. The maximum martensite content is 98.5 %, and there is also RA with a maximum content of 17.5 %. Bainite transformation mainly occurs in the J(5-16) region. In addition, due to the increase in the car-

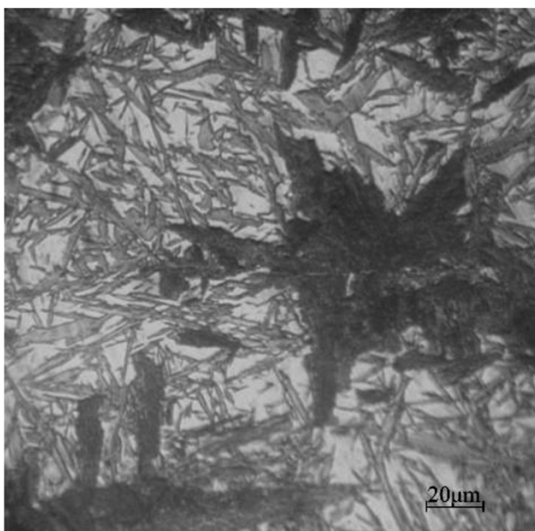


Figure 7: Surface microstructure of the Jominy sample

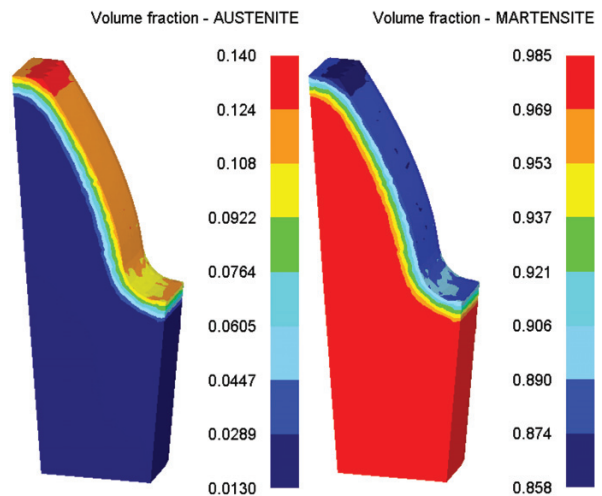


Figure 8: Phase transformation of the gear

bon content on the surface, the temperature of bainite transformation decreases, and bainite occurs on the surface in the region above J16, which corresponds to the TTT curve from Figure 2. Ferrite occurs in the core in the region above J16. As shown in Figure 7, the surface microstructure of the Jominy sample is mostly lower bainite, observed with an optical microscope, which is basically consistent with the simulated results. The phase transformation results of the gear are shown in Figure 8. Low-carbon and high-carbon martensite occur in the core and surface of the gear, respectively. In addition, there is still some RA on the surface. The content of RA at the addendum is the highest (14 %). The surface and core microstructures in Figure 9 are basically consistent with the simulation results.

#### 4.3 Hardness results

Figure 10 shows the hardness shaded display results and hardness curves of both models. The VFM hardness was calculated based on the carbon content and the content of each phase. The carbon contents at different

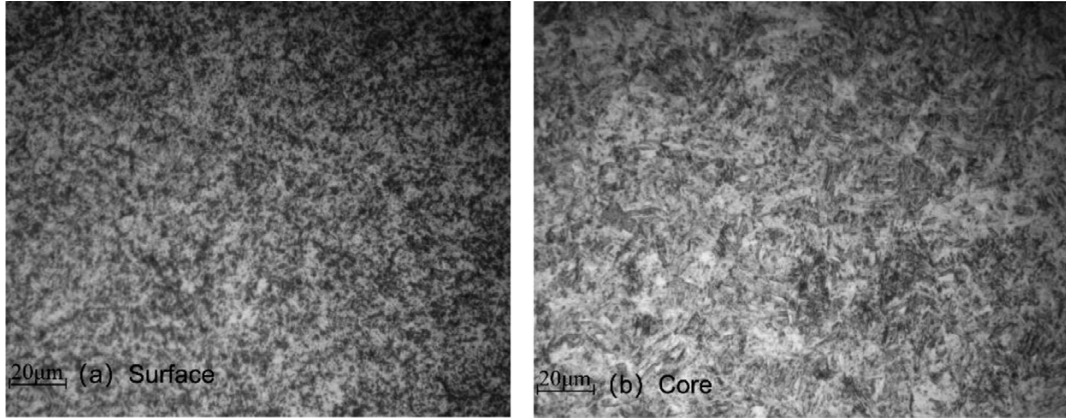


Figure 9: a) Surface and b) core microstructure of the gear

points and the phase transformations at different Jominy distances are different, so the hardness is also different. Martensite transformation mainly occurs in the J5 region. The hardness of the J5 region is the highest; the maximum hardness is 62.3 HRC, followed by the hardness in the J(5-16) region and on the surface in the region above J16 where the bainite transformation mainly occurs. The low hardness occurs in the residual region where the pearlite and ferrite transformations occur, and the minimum hardness is 17.1 HRC. Meanwhile, due to a different carbon content and phase transformation, there is a certain hardness gradient from the surface to the centre at the same Jominy distance. The JCM hardness is calculated based on the  $t_{8/5}$  and carbon content, which are different in the regions with different Jominy distances, so the hardness is also different. The water-cooled end has the minimum cooling time and a high carbon content, so the hardness is the largest and the maximum hardness is 64.3 HRC. At the same Jominy distance, the surface has a lower cooling time and a higher carbon content, so the hardness of the surface is higher. From the surface to the core, the cooling time increases and the carbon content decreases gradually, so the hardness also exhibits a certain gradient.

Similarly, due to different phase transformations, carbon contents and cooling times, a certain hardness gradient appears between the surface and the core of the gear. The maximum hardness of the gear in the VFM is 59.2 HRC and it is 63.5 HRC in the JCM. In summary, the carbon contents of both models are the same. The VFM must couple the results of the temperature and phase transformation, and then it calculates the hardness with the Maynier equation and Equation (11). The JCM determines the hardness only on the basis of the temperature result; this calculation process is more suitable. The maximum hardness obtained with the JCM is greater than that obtained with the VFM, regardless of the gear or Jominy sample. In Figure 3, the Jominy hardness increases with the increase in the carbon content; however, there is some RA during the quenching, which reduces the hardness. The JCM does not consider the influence of RA on the hardness, so the JCM hardness is higher

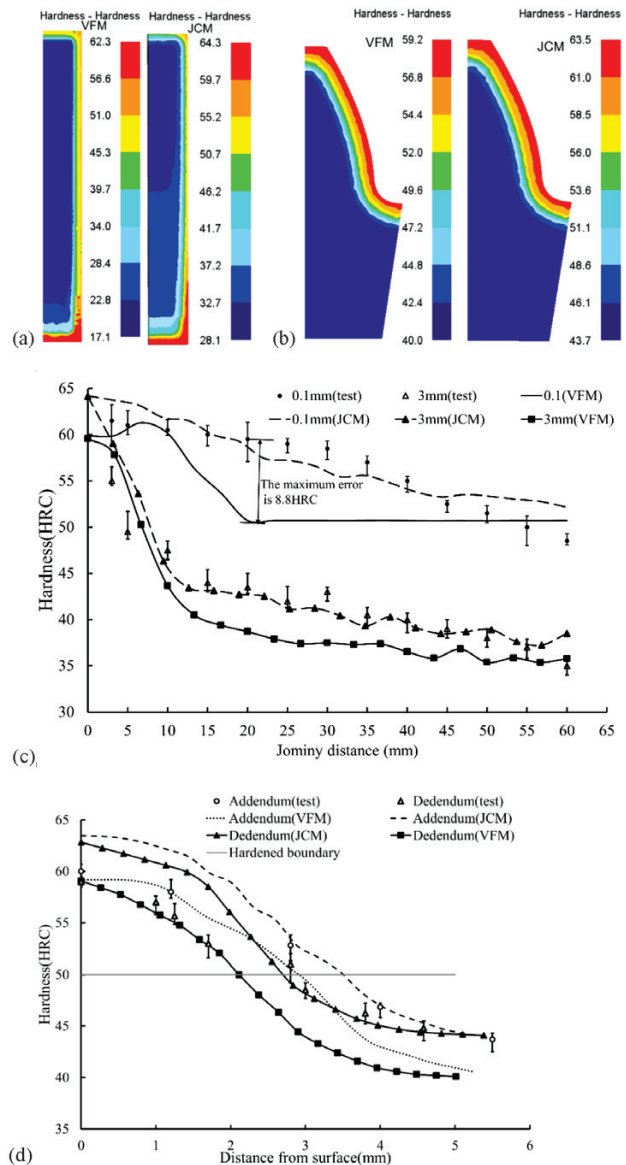


Figure 10: a) Hardness shaded display of the Jominy sample and b) the gear; c) hardness distribution curves of the Jominy sample and d) the gear

than that of the VFM in the regions on the surfaces of the Jominy and gear samples.

Compared with the experiment, the hardness values simulated by both models were generally consistent with the measured results, and the maximum error between the VFM and test hardness was 8.8 HRC. It showed that both models have a certain calculation accuracy. As the JCM did not consider the influence of RA on the hardness, the JCM hardness was higher than the test results in the curves of the region below J10, and the maximum error was 5 HRC, while the VFM hardness was basically in good agreement with the test results. In the region above J10, the simulation accuracy of the JCM was good, while the VFM hardness was smaller than the test result. The VFM needed to couple the results of the temperature and phase transformation; there were certain errors in the calculation of the diffusive phase transformation and Maynier equation. The JCM hardness could only be obtained based on the temperature field results, and the accumulated error was small, so the accuracy of the JCM was good. In the 3 mm hardness curve, the difference between both models was relatively small, mainly because the carbon content at this depth was 0.3 % and the hardness was less affected by the carbon content.

Similarly, taking 50 HRC as the boundary of case-hardening, the maximum error between the VFM hardness and the test results was only 3 %, and the accuracy of the VFM was higher than that of the JCM for case-hardening. The JCM hardness was higher than the test results, and the maximum error was 4.3 HRC. Outside the hardened case, the simulation accuracy of the VFM was higher than that of the JCM. This shows that the JCM hardness is more accurate than the hardness of low-carbon martensite calculated with the Maynier equation for the core, while the VFM hardness is more accurate for the hardened case.

## 5 CONCLUSIONS

(1) Unlike the conventional hardness models, a carburizing-quenching hardness model considers the influence of the carbon content on the phase transformation and hardness. In the VFM, the hardness of each phase was calculated with the Maynier equation and high-carbon martensite hardness equation, while the phase transformations were calculated with the KJMA and Koistinen-Marburger equations for different carbon contents. Jominy curves were obtained with an experiment, USS-Atlas formula and JmatPro for different carbon contents included in the JCM.

(2) By comparison with the test results, the VFM and JCM have a certain calculation accuracy. Due to considering the influence of RA on the hardness, the simulation accuracy of the VFM for the low Jominy distance and the hardened case was better than that of the JCM. The

maximum errors of the JCM were 5 HRC for the region below J10 and 4.3 HRC for the hardened case.

(3) Since only the temperature field needed to be calculated, the calculation of the JCM was more convenient and the accumulated error was small. The simulation accuracy of the JCM for the large Jominy distance and the low-carbon martensite region was better. Due to the limited calculation accuracy of the diffusive phase transformation and Maynier equation, the maximum errors of VFM were 8.8 HRC for the large Jominy distance and 3 % for the low-carbon martensite region.

## Acknowledgment

This work was supported by the Doctoral Cultivation Fund of the Henan University of Engineering (D2020004) and Science and Technology Research Project of the Henan Province (232102220041).

## 6 REFERENCES

- G. M. Chen, Review on carburizing and hardening technology of gears in China, *Heat Treatment of Metals*, 33 (2008), 25–33, doi:10.13251/j.issn.0254-6051.2008.01.007
- Z. X. Liu, X. D. Liu, F. J. Cao, W. L. Liu, C. H. Chen, R. M. Ren, Numerical simulation of structure field and hardness field on carburizing and quenching process of 20CrMnMo gear, *Hot Working Technology*, 42 (2013) 6, 204–207, doi:10.14158/j.cnki.1001-3814.2013.06.005
- D. Khan, B. Gautham, Integrated modeling of carburizing-quenching-tempering of steel gears for an ICME framework, *Integrating Materials and Manufacturing Innovation*, 7 (2018) 1, 28–41, doi:10.1007/s40192-018-0107-x
- X. H. Deng, D. Y. Ju, Modeling and simulation of quenching and tempering process in steels, *Physics Procedia*, 50 (2013), 368–374, doi:10.1016/j.phpro.2013.11.057
- J. Fluhner, DEFORM 2D-V9.0 and 3D-V6.0 User's Manual, Scientific Forming Technology Co., Columbus, 2005, 102
- D. V. Doane, J. S. Kirkalady, Hardenability concepts with applications to steel, *Metallurgical Society of AIME*, New York, 1978, 213
- P. R. Woodard, S. Chandraseker, H. T. Yang, Analysis of temperature and microstructure in the quenching of steel cylinders, *Metallurgical and Materials Transactions B*, 30 (1999), 815–822, doi:10.1007/s11663-999-0043-4
- J. Yuan, J. Kang, Y. Rong, R. Sisson, FEM modeling of induction hardening processes in steel, *Journal of Materials Engineering and Performance*, 12 (2003) 5, 589–596, doi:10.1361/105994903100277111
- X. Zhang, J. Y. Tang, An optimal hardness model for carburizing-quenching of low carbon alloy steel, *J. Cent. South Univ.*, 24 (2017) 1, 9–16, doi:10.1007/s11771-017-3403-2
- M. Schwenk, J. Hoffmeister, J. Hermes, Hardness prediction after case hardening and tempering gears as first step for a local load carrying capacity concept, *Forschung im Ingenieurwesen*, 81 (2017) 2, 233–243, doi:10.1007/s10010-017-0247-8
- X. Wang, B. K. Li, A carburizing-quenching Jominy curve hardness model, *Materials Letters*, 265 (2020), 127422, doi:10.1016/j.matlet.2020.127422
- D. H. Ko, D. C. Ko, H. J. Lim, B. M. Kim, Application of QFA coupled with CFD analysis to predict the hardness of T6 heat treated Al6061 cylinder, *Journal of Mechanical Science and Technology*, 27 (2013) 9, 2839–2844, doi:10.1007/s12206-013-0732-4

- <sup>13</sup> M. Kianezhad, S. A. Sajjadi, Improvement of quench factor analysis in phase and hardness prediction of a quenched steel, *Metallurgical and Materials Transactions A*, 44 (2013) 5, 2053–2059, doi:10.1007/s11661-012-1574-x
- <sup>14</sup> P. A. Rometsch, M. J. Starink, P. J. Gregson, Improvements in quench factor modelling, *Mater. Sci. Eng.: A*, 339 (2003) 1, 255–264, doi:10.1016/S0921-5093(02)00110-7
- <sup>15</sup> M. Kianezhad, S. A. Sajjadi, H. Vafaenezhad, A numerical approach to the prediction of hardness at different points of a heat-treated steel, *Journal of Materials Engineering and Performance*, 24 (2015) 4, 1516–1521, doi:10.1007/s11665-015-1433-1
- <sup>16</sup> A. X. Wang, J. Z. Gao, M. Gu, Heat treatment of new type high alloy carburizing gear steel 17CrNiMo6, *Heat Treatment of Metals*, 35 (2010) 10, 82–86, doi:10.13251/j.issn.0254-6051.2010.10.021
- <sup>17</sup> X. Zhang, J. Y. Tang, Key technology in carburizing process simulation for 17CrNiMo6 steel annular gear, *Heat Treatment of Metals*, 40 (2015) 3, 185–189, doi:10.13251/j.issn.0254-6051.2015.03.042
- <sup>18</sup> D. W. Kim, Y. G. Cho, H. H. Cho, S. H. Kim, W. B. Lee, M. G. Lee, H. N. Han, A numerical model for vacuum carburization of an automotive gear ring, *Metals & Materials International*, 17 (2011) 6, 885–890, doi:10.1007/s12540-011-6004-x
- <sup>19</sup> D. Khan, R. Shukla, B. P. Gautham, In silico design of materials and processes: an application of ICME to carburizing steels, *Transactions of The Indian Institute of Metals*, 72 (2019), 2179–2185, doi:10.1007/s12666-018-1534-2
- <sup>20</sup> M. Hadhri, A. El Ouafi, N. Barka, Prediction of the hardness profile of an AISI 4340 steel cylinder heat-treated by laser – 3D and artificial neural networks modelling and experimental validation, *Journal of Mechanical Science and Technology*, 31 (2017) 2, 615–623, doi:10.1007/s12206-017-0114-4
- <sup>21</sup> A. Sugianto, M. Narazaki, M. Kogawara, A. Shirayori, S. Y. Kim, S. Kubota, Numerical simulation and experimental verification of carburizing-quenching process of SCr420H steel helical gear, *Journal of Materials Processing Technology*, 209 (2009) 7, 3597–3609, doi:10.1016/j.jmatprotec.2008.08.017
- <sup>22</sup> C. C. Liu, X. J. Xu, Z. Liu, A FEM modelling of quenching and tempering and its application in industrial engineering, *Finite Elements in Analysis and Design*, 39 (2003) 11, 1053–1070, doi:10.1016/S0168-874X(02)00156-7
- <sup>23</sup> Y. Liu, S. W. Qin, Q. G. Hao, N. L. Chen, X. W. Zuo, Y. H. Rong, Finite element simulation and experimental verification of internal stress of quenched AISI 4140 cylinders, *Metallurgical & Materials Transactions A*, 48 (2017) 3, 1402–1413, doi:10.1007/s11661-016-3916-6
- <sup>24</sup> A. S. Oddy, J. M. J. McDill, Numerical prediction of microstructure and hardness in multicycle simulations, *Journal of Materials Engineering and Performance*, 5 (1996) 3, 365–372, doi:10.1007/BF02649338
- <sup>25</sup> S. J. Lee, K. S. Park, Prediction of martensite start temperature in alloy steels with different grain sizes, *Metallurgical & Materials Transactions A*, 44 (2013) 8, 3423–3427, doi:10.1007/s11661-013-1798-4
- <sup>26</sup> B. B. Yu, *Computer designer of steel*, Metallurgical Industry Press, Beijing 1996
- <sup>27</sup> M. Gu, B. K. Li, A. X. Wang, S. F. Zhao, H. X. Xu, Q. Y. Zhu, Study on the heat treatment distortion characteristics of the typical carburizing and hardening gear steel, 9th national heat treatment conference, Dalian, China, 2007, 142–148
- <sup>28</sup> A. Sugianto, M. Narazaki, M. Kogawara, Distortion analysis of axial contraction of carburized-quenched helical gear, *Journal of Materials Engineering and Performance*, 19 (2010) 2, 194–206, doi:10.1007/s11665-009-9476-9